MONTANA STATE UNIVERSITY

Arsenate mobility through a saturated sand : effects of pore water velocity, PH and phosphate competition
by Jeffrey Edwin Darland

A thesis submitted in partial fulfillment of the requirements for the degree of Master of Science in Environmental Engineering
Montana State University
© Copyright by Jeffrey Edwin Darland (1996)

Abstract:
Previous studies have indicated that sorption of ASO4 onto soil mineral phases may be kinetically limited by diffusional processes, and other studies have demonstrated some of the effects of pH and PO4 competition on the sorption of AsO4 onto soil mineral phases. However, these studies have typically been performed in well-mixed batch systems, and it is unclear the extent to which data derived from batch experiments may be extrapolated to a transport condition. Consequently, the objective of this study was to determine the effects of pore water velocity, pH, and PO4 competition on the transport of AsO4 through a model sand where the principle reactive phase was amorphous or poorly crystalline Fe-oxides. The convection-dispersion equation (CDE) was used to predict the saturated transport of AsO4 through the sand at four different pore water velocities (PWVs) using equilibrium and kinetic expressions to describe the sorption of AsO4 by the sand. Saturated column transport experiments were performed using an applied AsO4 pulse (133 pM) through a disturbed sand at PWVs of 0.2, 1.0, 10, and 90 cm h^-1 (pH=4.5). In addition, saturated transport studies were performed in the presence of 0, 13.4, 134, and 1340 pM PO4, at pH values of 4.5, 6.5, and 8.5 (PWV=1 cm h^-1).

Observed AsO4 breakthrough curves (BTCs) demonstrated sorption related nonequilibrium at pH=4.5 at all PWVs. The use of independently derived equilibrium and kinetic sorption parameters (batch) in the CDE failed to describe observed BTCs at all PWVs. Fitting of kinetic rate parameters in the CDE to the observed BTCs resulted in different apparent sorption rate parameters at each PWV modeled. Enhanced mobility of AsO4 at pH=8.5 was identified as a pH effect. PO4 competition resulted in increased AsO4 mobility, however even in the presence of excess PO4 significant amounts of AsO4 remained sorbed to the sand. The indication is that AsO4 desorption kinetics play an important role in transport of AsO4 through porous media. Furthermore, sorption rates of AsO4 during transport appear to be highly dependent upon PWV, suggesting that kinetic data obtained from batch studies may not be extrapolatable to all transport conditions.

ARSENATE MOBILITY THROUGH A SATURATED SAND: EFFECTS OF PORE WATER VELOCITY, pH AND PHOSPHATE COMPETITION

by

Jeffrey Edwin Darland

A thesis submitted in partial fulfillment
of the requirements for the degree

of

Master of Science

in

Environmental Engineering

MONTANA STATE UNIVERSITY
Bozeman, Montana

January 1996

© COPYRIGHT

by

Jeffrey Edwin Darland

1996

All Rights Reserved

N378
D2489

APPROVAL

of a thesis submitted by

Jeffrey Edwin Darland

This thesis has been read by each member of the thesis committee and has been found to be satisfactory regarding content, English usage, format, citations, bibliographic style, and consistency, and is ready for submission to the College of Graduate Studies.

Jan 16, 1996
Date

Otto R Stein
Chairperson, Graduate Committee

Approved for the Major Department

1/16/96
Date

Robert L. Oakberg
Head, Major Department

Approved for the College of Graduate Studies

2/10/96
Date

RL Brown
Graduate Dean

STATEMENT OF PERMISSION TO USE

In presenting this thesis in partial fulfillment of the requirements for a master's degree at Montana State University, I agree that the Library shall make it available to borrowers under rules of the Library.

If I have indicated my intention to copyright this thesis by including a copyright notice page, copying is allowable only for scholarly purposes, consistent with "fair use" as prescribed in the U.S. Copyright Law. Requests for permission for extended quotation from or reproduction of this thesis in whole or in parts may be granted only by the copyright holder.

Signature Jeffrey E [illegible]/ORS

Date Jan 16, 1996

ACKNOWLEDGMENTS

I would not have been able to complete this work without the support of others. I would like to thank Dr. William Inskeep, Dr. Hesham Gaber, and Dr. Jon Wraith for their help and support in this work. I would also like to thank Dr. Otto Stein, without whose support I never would have made it out to Montana State University, and Dr. Warren Jones for serving as a member of my graduate committee.

I would also like to thank Clain Jones, Heiko Langner, Dr. Shaobai Sun, and Rich Macur, who were forced to share both a lab and their knowledge.

Finally, I would like to thank my parents, Paula Larson and Lawrence Stein, and my wife, Colette, for all of the love and support given to me during this endeavor.

TABLE OF CONTENTS

LIST OF TABLES vii

LIST OF FIGURES viii

ABSTRACT x

1. INTRODUCTION 1

2. EFFECTS OF PORE WATER VELOCITY ON THE TRANSPORT OF AsO_4 THROUGH A SAND 3

- 2.1. Introduction 4
- 2.2. Transport Model Formulations 6
  - 2.2.1. Equilibrium Partitioning Models 8
  - 2.2.2. Non-Equilibrium Partitioning Models 8
- 2.3. Materials and Methods 10
  - 2.3.1. Reagents and Analysis 10
  - 2.3.2. Kinetic Adsorption Study 11
  - 2.3.3. Batch Isotherms 12
  - 2.3.4. Column Transport Experiments 12
  - 2.3.5. Determination of Column Transport Parameters 13
- 2.4. Results 14
  - 2.4.1. Kinetic Adsorption Study 14
  - 2.4.2. Batch Adsorption Isotherms 15
  - 2.4.3. Determination of Kinetic Adsorption/Desorption Rate Parameters 15
  - 2.4.4. Column Transport Experiments 17
  - 2.4.5. Predicted Breakthrough Curves - LEA 20
  - 2.4.6. Predicted Breakthrough Curves - Kinetic Reversible Sorption 22
  - 2.4.7. Fitted Breakthrough Curves - nth-order kinetic 24
- 2.5. Discussion 27
- 2.6. Conclusions 29
- 2.7. Nomenclature 31

TABLE OF CONTENTS - Continued

3. EFFECTS OF pH AND PHOSPHATE COMPETITION ON THE TRANSPORT OF AsO_4 THROUGH A SAND 32

3.1. Introduction 33

3.2. Materials and Methods 35
  3.2.1. Reagents and Analysis 35
  3.2.2. Kinetic Adsorption Study 36
  3.2.3. Batch Isotherms 37
  3.2.4. Column Transport Experiments 37
  3.2.5. Determination of Column Transport Parameters 40

3.3. Results and Discussion 41
  3.3.1. Batch Adsorption 41
  3.3.2. Effects of pH on As Transport 44
  3.3.3. Effects of Phosphate Competition on As Transport 50

3.4. Conclusions 55

4. CONCLUSIONS AND GENERAL DISCUSSION 56

4.1. Implications for Modeling 58

4.2. Implications for Soil Liming 62

4.3. Implications for PO_4 Application 62

5. REFERENCES 64

LIST OF TABLES

Table 1: Sorbed phase accumulation terms used in the basic convection-dispersion equation (CDE) 7

Table 2: Physical and chemical characteristics of sand used. Surface area determined by triple point BET N_2 isotherms. Total chemical composition determined by Li-metaborate fusion. "Free" Al and Fe determined by citrate-dithionite (C-D) extraction. Numbers in parentheses indicate standard deviation of three samples. 10

LIST OF FIGURES

Figure 1: Adsorption kinetics of AsO_4 onto sand and FITMRM model results for first- and nth-order kinetic models. Experimental conditions: 1:1 solid:solution ratio (5 g (dry weight) solid:5 mL solution); pH range = 4 to 5; 150 μM initial AsO_4 in a background solution of 0.01 M KCl.......... 14

Figure 2: Adsorption isotherms (Background: 0.01 M KCl) for AsO_4 at a 1:2 solid:solution ratio (5 g (dry weight) solid:10 mL solution) and a pH range of 4.0 to 4.6. Fitted lines represent (i) the linear isotherm using an approximate K_D of 200 L kg^{-1} to fit the linear portion of the data, and (ii) the Freundlich isotherm where K_F and 1/n were fit using nonlinear regression.......... 16

Figure 3: Observed and predicted (CXTFIT) ^3H_2O breakthrough curves at three different pore water velocities (1, 10, and 90 cm h^{-1}). Column conditions: Background = 0.01 M KCl; ^3H_2O pulse = 1 pore volume.......... 18

Figure 4: Observed AsO_4 breakthrough curves to 10 pore volumes, at four different pore water velocities (PWVs) (0.2, 1, 10, and 90 cm h^{-1}). Column conditions: Background = 0.01 M KCl; AsO_4 pulse = 1 pore volume at 133 μM.......... 19

Figure 5: Predicted (MRTM) AsO_4 distribution in sand columns after 50 pore volumes total flow under the LEA using independent estimates of linear (——) and Freundlich (- - -) adsorption parameters and dispersion coefficients from ^3H_2O BTCs (column conditions: background = 0.01 M KCl; AsO_4 pulse = 1 pore volume at 133 μM): (a) pore water concentration; (b) sorbed phase concentration.......... 21

Figure 6: Observed (×) and predicted AsO_4 BTCs (MRTM) for first (- - -) and nth-order (——) kinetic adsorption expressions at three different pore water velocities (PWVs) using kinetic parameters derived from batch experiments (column conditions: background = 0.01 M KCl; AsO_4 pulse = 1 pore volume at 133 μM): (a) PWV=1 cm h^{-1}; (b) PWV=10 cm h^{-1}; (c) PWV=90 cm h^{-1}.......... 23

Figure 7: Observed (×) and fitted (——) AsO_4 breakthrough curves (BTCs) obtained by optimizing rate parameters (k_f, k_r, n) of the nth-order kinetic adsorption expression at three different pore water velocities (PWVs). Predicted (- - -) AsO_4 BTCs are shown for 10 and 90 cm h^{-1} PWV treatments using fitted rate parameters determined at 1 cm h^{-1} (column conditions: background = 0.01 M KCl; AsO_4 pulse = 1 pore volume at 133 μM): (a) PWV=1 cm h^{-1}; (b) PWV=10 cm h^{-1}; (c) PWV=90 cm h^{-1}.......... 26

LIST OF FIGURES - Continued

Figure 8: Adsorption kinetics of AsO_4 and PO_4 onto sand (single ion experiment) at a 1:1 solid:solution ratio (5 g (dry weight) solid:5 mL solution and at pH values ranging from 4 to 5 (AsO_4) and 4 to 5.7 (PO_4)). Initial concentrations were 150 µM AsO_4 and 360 µM PO_4 in a background solution of 0.01 M KCl. 42

Figure 9: Adsorption isotherms (0.01 M KCl) for AsO_4 in the absence and presence of 134 µM and 1340 µM PO_4 at a 1:1 solid:solution ratio (15 g (dry weight) solid:15 mL solution) and a pH range of 4.0 to 4.6. Solid lines represent best fit Langmuir isotherms, where Γ_0 = maximum adsorption density and K_L = empirical affinity parameter. 43

Figure 10: The transport of AsO_4 through a sand at three different carbonate buffered pH values: 4.5, 6.5 and 8.5 (Column conditions: Pore water velocity = 1 cm h^{-1}; Background = 0.01 M KCl; AsO_4 pulse = 1 pore volume at 133 µM)....... 45

Figure 11: The transport of AsO_4 through clean quartz sand (Fluka) at pH 7 (Column conditions: Pore water velocity = 1 cm h^{-1}; Background = 0.01 M KCl; AsO_4 pulse = 1 pore volume at 133 µM). 46

Figure 12: The distribution of AsO_4 species (solid lines represent concentration, dashed lines represent activity) as a function of pH for conditions specific to the column experiments (0.01 M KCl, 133 µM AsO_4); based on: pK_{a1}=2.24, pK_{a2}=6.94, pK_{a3}=11.5 (Sadiq et al., 1983). 48

Figure 13: The transport of AsO_4 through sand at pH 8.5 in the presence and absence of CO_2(g) buffering (Column conditions: Pore water velocity = 1 cm h^{-1}; Background = 0.01 M KCl; AsO_4 pulse = 1 pore volume at 133 µM). 49

Figure 14: The transport of AsO_4 through sand at pH 4.5 in the presence of 0, 13.4, 134, and 1340 µM PO_4 (Column conditions: Pore water velocity = 1 cm h^{-1}; Background = 0.01 M KCl; AsO_4 pulse = 1 pore volume at 133 µM). 50

Figure 15: The transport of AsO_4 through sand at pH 6.5 (CO_2(g) buffered) in the presence of 0, 13.4, 134, and 1340 µM PO_4 (Column conditions: Pore water velocity = 1 cm h^{-1}; Background = 0.01 M KCl; AsO_4 pulse = 1 pore volume at 133 µM). 51

Figure 16: The transport of AsO_4 through sand at pH 4.5 followed by continuous addition of 1420 µM PO_4 at ~20 pore volumes (Column conditions: Pore water velocity = 1 cm h^{-1}; Background = 0.01 M KCl; AsO_4 pulse = 1 pore volume at 143 µM). 53

ABSTRACT

Previous studies have indicated that sorption of AsO_4 onto soil mineral phases may be kinetically limited by diffusional processes, and other studies have demonstrated some of the effects of pH and PO_4 competition on the sorption of AsO_4 onto soil mineral phases. However, these studies have typically been performed in well-mixed batch systems, and it is unclear the extent to which data derived from batch experiments may be extrapolated to a transport condition. Consequently, the objective of this study was to determine the effects of pore water velocity, pH, and PO_4 competition on the transport of AsO_4 through a model sand where the principle reactive phase was amorphous or poorly crystalline Fe-oxides. The convection-dispersion equation (CDE) was used to predict the saturated transport of AsO_4 through the sand at four different pore water velocities (PWVs) using equilibrium and kinetic expressions to describe the sorption of AsO_4 by the sand. Saturated column transport experiments were performed using an applied AsO_4 pulse (133 μM) through a disturbed sand at PWVs of 0.2, 1.0, 10, and 90 cm h^{-1} (pH=4.5). In addition, saturated transport studies were performed in the presence of 0, 13.4, 134, and 1340 μM PO_4, at pH values of 4.5, 6.5, and 8.5 (PWV=1 cm h^{-1}). Observed AsO_4 breakthrough curves (BTCs) demonstrated sorption related nonequilibrium at pH=4.5 at all PWVs. The use of independently derived equilibrium and kinetic sorption parameters (batch) in the CDE failed to describe observed BTCs at all PWVs. Fitting of kinetic rate parameters in the CDE to the observed BTCs resulted in different apparent sorption rate parameters at each PWV modeled. Enhanced mobility of AsO_4 at pH=8.5 was identified as a pH effect. PO_4 competition resulted in increased AsO_4 mobility, however even in the presence of excess PO_4 significant amounts of AsO_4 remained sorbed to the sand. The indication is that AsO_4 desorption kinetics play an important role in transport of AsO_4 through porous media. Furthermore, sorption rates of AsO_4 during transport appear to be highly dependent upon PWV, suggesting that kinetic data obtained from batch studies may not be extrapolatable to all transport conditions.

1. INTRODUCTION

Arsenic (As) is an important contaminant in many reclamation sites containing fly ash and mining waste, and exists in elevated concentration in soils impacted by natural and geothermal sources (e.g., Madison River Valley, Montana) (Sonderegger and Ohguchi, 1988) as well. Since As presents a significant health hazard in groundwaters used for domestic purposes, there is a need to understand processes affecting As transport in soils, sediments, and aquifers, especially in regions where groundwater is a principle source of domestic drinking water.

There has been substantial previous research on processes affecting As (as AsO_4) sorption by soils and soil mineral phases. Such research has included kinetic studies of adsorption onto oxide mineral phases (e.g. Grossl, 1995; Fuller et al., 1993), the effects of pH on sorption (e.g. Anderson, et al., 1976; Pierce and Moore, 1982; Goldberg, 1986; Hingston et al., 1971), and the effects of anion competition with phosphate (PO_4) during sorption (e.g. Hingston et al., 1971; Goldberg, 1986; Peryea, 1991); and these processes have been successfully quantified and modeled in batch systems. It is unclear, however, the extent to which batch derived data (typically involving well-mixed low solid:solution ratios) may be extrapolated to transport environments, particularly as regards coupling these processes with existing transport models.

This thesis comprises two studies designed to elucidate factors affecting As transport (as AsO_4) through saturated soils and aquifers. In particular, Chapter 2 investigates the effect of pore water velocity and subsequent kinetic limitations that can occur during AsO_4 transport. The role of soil water pH and PO_4 competition on the transport of AsO_4 is investigated in Chapter 3. The objectives of the current studies were to determine:

(i) the applicability of batch derived equilibrium and kinetic partitioning parameters in transport models describing AsO_4 transport through a representative sand,

(ii) the effects of pore water velocity on sorption rate coefficients derived during AsO_4 transport,

(iii) the effect of pH on AsO_4 transport,

(iv) the extent to which simultaneous competition between AsO_4 and PO_4 for adsorption sites affects AsO_4 transport,

(v) the effect of pH on the competition between AsO_4 and PO_4 for adsorption sites during transport, and

(vi) the extent to which modification of pore water PO_4 concentration could increase AsO_4 mobility in contaminated aquifer sands.

2. EFFECTS OF PORE WATER VELOCITY ON THE TRANSPORT OF AsO_4 THROUGH A SAND

Previous studies have shown that the sorption of AsO_4 by Fe- and Al-oxide minerals may be kinetically limited by diffusional processes even under well-mixed batch conditions. The potential for AsO_4 to exhibit sorption related nonequilibrium during transport has not been previously determined. Consequently, the objectives of this study were to determine the applicability of transport models based on the convection-dispersion equation (CDE) using equilibrium (linear and Freundlich) and kinetic (first- and nth-order) sorption expressions in describing AsO_4 mobility. Saturated column transport experiments were performed using an applied AsO_4 pulse (1 pore volume, 133 µM $^{73}AsO_4$) at pore water velocities (PWVs) of 0.2, 1.0, 10, and 90 cm h^{-1} through a sand where the principle reactive phase was amorphous or poorly crystalline Fe-oxides. Observed AsO_4 breakthrough curves (BTCs) exhibited poor recovery and significant tailing at all pore water velocities, and demonstrated sorption related nonequilibrium as evidenced by a leftward shift in observed BTCs and an increase in observed effluent recovery with increasing PWV. The use of independently derived equilibrium and kinetic sorption parameters (batch) and column dispersion coefficients (from ^3H_2O BTCs) in the CDE failed to describe observed AsO_4 BTCs at all pore water velocities. Rate parameters obtained by fitting observed BTCs to the nth-order kinetic model resulted in different apparent sorption rate coefficients and isotherm nonlinearity parameters as a function of PWV. Fitted apparent adsorption and desorption rate coefficients increased with increasing PWV. The results of this study indicate that sorption rates of AsO_4 onto soils and aquifer materials during transport are highly dependent upon pore water velocity, and that kinetic data obtained from batch studies cannot be readily extrapolated to all transport conditions.

2.1. Introduction

The two principle forms of As in groundwaters are AsO_3 (As(III)) and AsO_4 (As(V)). Under oxidizing environments where AsO_4 is generally predominant relative to AsO_3, and solution concentrations of AsO_4 do not exceed the solubility product of metal arsenate solid phases, soluble equilibrium AsO_4 concentrations can be expected to be controlled by adsorption onto mineral surfaces. Moreover, AsO_4 is generally preferentially sorbed to metal oxide surfaces compared to layer silicates (Fordam and Norrish, 1979; Jacobs et al., 1970; Johnson and Barnard, 1979; Livesey and Huang, 1981; Fuller et al., 1993). Arsenate adsorption by Fe hydroxides can be categorized as a ligand exchange mechanism, and it has been shown by Extended X-ray Absorption Fine Structure Spectroscopy (EXAFS) that AsO_4 forms a combination of mono- and bidentate complexes with surface Fe sites (Waychunas et al., 1993). For AsO_4 adsorption onto α-FeOOH, these ligand exchange reactions have been represented by (Goldberg, 1986; Grossl, 1995):

$$\begin{aligned}
\mathrm{FeOH(s)} + \mathrm{H_3AsO_4(aq)} &= \mathrm{FeH_2AsO_4(s)} + \mathrm{H_2O} \\
\mathrm{FeOH(s)} + \mathrm{H_3AsO_4(aq)} &= \mathrm{FeHAsO_4^{-}(s)} + \mathrm{H_2O} + \mathrm{H^+(aq)} \\
\mathrm{FeOH(s)} + \mathrm{H_3AsO_4(aq)} &= \mathrm{FeAsO_4^{2-}(s)} + \mathrm{H_2O} + \mathrm{2H^+(aq)} \\
\mathrm{2FeOH(s)} + \mathrm{H_3AsO_4(aq)} &= \mathrm{Fe_2HAsO_4(s)} + \mathrm{2H_2O} \\
\mathrm{2FeOH(s)} + \mathrm{H_3AsO_4(aq)} &= \mathrm{Fe_2AsO_4^{-}(s)} + \mathrm{2H_2O} + \mathrm{H^+(aq)}
\end{aligned}$$

and have successfully described equilibrium sorption conditions over the pH range of 3.5 to 10 using the Constant Capacitance model.

The actual chemical step describing the surface complexation of AsO_4 onto Fe oxides and clay minerals is quite rapid, generally on the order of milliseconds (Grossl, 1995; Amacher, 1991; Sparks and Zhang, 1991). Studies have shown, however, that even in well-mixed batch systems the approach to equilibrium can be slow, on the order of hours, for AsO_4 adsorption onto amorphous Al-hydroxides (Anderson et al., 1976) and ferrihydrite (Fuller et al., 1993). These results indicate that mass transfer limitations such as interparticle, intraparticle, and film diffusion may play a significant role in the kinetics of AsO_4 sorption onto soil minerals phases (Fuller et al., 1993). The extent to which these kinetic processes may affect the transport of AsO_4 through soils and/or aquifer materials is unclear.

Sorption processes influenced by slow mass transfer rates may be subject to chemical (sorption related) nonequilibrium under transport conditions (Brusseau, 1992). Under these situations, it is characteristic to observe changes in the shape (e.g. tailing) of solute breakthrough curves as a function of pore water velocity (Bouchard et al., 1988; Brusseau, 1992; Gaber et al., 1992; Gaber et al., 1995). Moreover, transport derived rate constants representing the adsorption/desorption process may vary with pore water velocity (Gaber et al., 1995; Brusseau, 1992; Gamerdinger et al., 1991), indicating that the diffusional processes controlling adsorption/desorption rates are sensitive to the mixing environment (Ball et al., 1991).

While there has been substantial research on batch equilibrium sorption reactions of AsO_4 onto geological minerals and natural soils, there have been few studies investigating the role of kinetic limitations on AsO_4 sorption by soils. Furthermore, there is a lack of detailed data on the effects of kinetic processes on AsO_4 transport through porous media. The primary goal of the current study was to elucidate the adsorption effects and kinetic limitations on AsO_4 transport through a saturated sand. In particular, the objectives were to (i) determine the applicability of two equilibrium adsorption models (linear and Freundlich) and two simple kinetic adsorption models (first-order and nth-order reversible) in describing AsO_4 transport using the convection-dispersion equation (CDE), and (ii) to determine the effect of pore water velocity on apparent sorption rate coefficients derived during As transport.

2.2. Transport Model Formulations

The convection-dispersion equation (CDE) describes the one-dimensional steady-state transport of adsorbing solutes through soils:

$$\rho\frac{\delta s}{\delta t}+\theta\frac{\delta c}{\delta t}=\theta\cdot D\frac{\delta^2 c}{\delta x^2}-v\frac{\delta c}{\delta x} \qquad (1)$$

where ρ represents soil bulk density [M L^{-3}], s represents sorbed concentration [M M^{-1}], t represents time [T], θ represents volumetric water content [L^3 L^{-3}], c represents solute concentration [M L^{-3}], D represents the hydrodynamic dispersion coefficient [L^2 T^{-1}], v represents average pore water velocity [L T^{-1}], and x represents distance [L]. The left side of this mass-balance equation represents the accumulation of solute in the sorbed ($\delta s/\delta t$) and liquid ($\delta c/\delta t$) phases, while the right side represents mass flux of solute due to dispersion and convection.

Travis and Etnier (1981) provided a fairly comprehensive review of the relationships used to quantify adsorption of reactive solutes by soils. Fundamentally, the adsorption of solutes can be modeled as either an equilibrium or a kinetic process, depending on whether or not the sorbed phase is locally at equilibrium with the resident solution phase concentration. Common equilibrium and kinetic expressions used to describe the change in sorbed phase concentration ($\delta s/\delta t$) in the CDE are presented in Table 1, corresponding to adsorption described by both the linear and the Freundlich isotherms, where K_D, K_F, K_D', and K_F' are distribution coefficients [L^3 M^{-1}], k_f is a forward reaction rate constant [T^{-1}], k_r is a reverse reaction rate constant [T^{-1}], and n is a dimensionless Freundlich reaction order.

Table 1: Sorbed phase accumulation terms used in the basic convection-dispersion equation (CDE).

	Model	Sorbed Phase Accumulation Term	Partitioning at Equilibrium
Case A.	Linear Equilibrium	$\frac{\delta s}{\delta t} = K_D \cdot \frac{\delta c}{\delta t}$	$s = K_D \cdot c$
Case B.	Freundlich Equilibrium	$\frac{\delta s}{\delta t} = \frac{K_F}{n} c^{(1/n - 1)} \cdot \frac{\delta c}{\delta t}$	$s = K_F \cdot c^{1/n}$
Case C.	First-Order Reversible	$\frac{\delta s}{\delta t} = \frac{\theta}{\rho} k_f c - k_r s$	$s = K_D' \cdot c$ $K_D' = \frac{\theta}{\rho} \frac{k_f}{k_r}$
Case D.	nth-Order Reversible	$\frac{\delta s}{\delta t} = \frac{\theta}{\rho} k_f c^{1/n} - k_r s$	$s = K_F' \cdot c^{1/n}$ $K_F' = \frac{\theta}{\rho} \frac{k_f}{k_r}$

2.2.1. Equilibrium Partitioning Models

It is often assumed that the resident solution phase concentration is locally at equilibrium with the sorbed phase concentration (defined as the Local Equilibrium Assumption, LEA). Solutions to the CDE using the LEA have employed the linear isotherm (e.g., Lapidus and Amundson, 1952) (Table 1, Case A) and the Freundlich isotherm (Sidle et al., 1977, Bahr and Rubin, 1987; Selim et al., 1990) (Table 1, Case B). One of the principle benefits of these expressions is that the adsorbed solute concentration can be described solely as a function of soluble concentration, which greatly simplifies the numerically integrated solution of the CDE. There have been many published reports, however, which indicate that nonequilibrium conditions during transport preclude the use of the LEA with either linear or Freundlich isotherms (Valocchi, 1985; Parker and Valocchi, 1986; Bahr and Rubin, 1987; Gaber et al., 1992).

2.2.2. Non-Equilibrium Partitioning Models

Transport models based on the CDE using kinetic expressions to describe adsorption processes have also been previously published (van Genuchten et al., 1974; Sparks and Jardine, 1984; Bahr and Rubin 1987; Selim et al., 1990). The simplest kinetic expression is a first-order reversible reaction (Table 1, Case C), which at equilibrium corresponds to a linear isotherm (Sparks and Jardine, 1984; Bahr and Rubin 1987). Kinetic expressions describing nth-order reversible adsorption (which at equilibrium reduces to the Freundlich isotherm) have also been used in the CDE (Table 1, Case D) (e.g. van Genuchten et al., 1974; Bahr and Rubin, 1987; Selim et al., 1990). Additional approaches for modeling nonequilibrium conditions during the transport of reactive solutes include defining different sorption domains. For example, the two site nonequilibrium model (Cameron and Klute, 1977; Parker and van Genuchten, 1984; Brusseau et al., 1991) assumes instantaneous sorption in one domain and rate limited sorption in another domain (rate limited sorption described by the first-order reversible reaction). Selim et al. (1990) considered the soil system as a complex combination of up to five different types of reaction sites (domains) including equilibrium reversible Freundlich, kinetic nth-order reversible, and kinetic nth-order irreversible adsorption.

If any transport model is to be used in a predictive role, a certain number of input parameters must be obtained independently from external sources. Common sources of this information include laboratory batch studies or tabulated literature values. Generally, the number of required input parameters increases with model complexity. In a practical sense, minimization of the complexity of the input requirements is desired. While previous work has been directed toward assessing the applicability of particular models, most of this previous work is directed toward the applicability of the LEA (e.g. Valocchi, 1985; Parker and Valocchi, 1986; Bahr and Rubin, 1987; Gaber et al., 1992) and the existing literature has focused primarily on the transport of organic or heavy metal contaminants. Few studies have been directed toward the applicability of these models to the transport of AsO_4, which is an important contaminant in soils, aquifers, and surface waters. Moreover, the extent to which batch derived equilibrium and/or kinetic parameters may be useful for predicting AsO_4 transport is unclear.

2.3. Materials and Methods

2.3.1. Reagents and Analysis

Sand of mixed mineralogy was obtained from the Unimin Corporation, Emmett, Idaho (Granusil Grade 50), sieved to a particle size range of 0.25 to 0.50 mm, acid washed with 0.05 M HCl (3 times), then rinsed with double deionized water (DD-H_2O) until the conductivity of the rinse stabilized at <2μS. The sand was then oven dried at 105°C, and characterized for surface area (SA), cation exchange capacity (CEC), amorphous Fe and Al hydroxides by citrate-dithionite extraction (Olson and Ellis, 1982), and chemical composition by total dissolution (Table 2).

Table 2: Physical and chemical characteristics of sand used. Surface area determined by triple point BET N_2 isotherms. Total chemical composition determined by Li-metaborate fusion. "Free" Al and Fe determined by citrate-dithionite (C-D) extraction. Numbers in parentheses indicate standard deviation of three samples.

Element	%-by weight	Deviation
Si	36.798	(0.454)
K	4.044	(0.414)
Al	3.764	(0.251)
Ca	0.570	(0.035)
Na	0.311	(0.086)
Fe	0.054	(0.025)
Mn	< 0.002	
P	< 0.002	
Fe-"Free"	0.010	(0.001)
Al-"Free"	< 0.010	

Particle Size: 0.25 to 0.50 mm - seived
Surface Area: 0.390 ± 0.034 m^2/g
CEC: 2.7 x 10^{-3} mmol charge/g

All AsO_4 solutions were prepared with the same source of analytical grade Na_2HAsO_4 salt (Baker), and diluted with DD-H_2O. Solution AsO_4 concentrations were measured by three different methods depending on the experiments performed. For batch studies, AsO_4 was measured by atomic absorption with continuous hydride generation (AA-HG). For transport studies, radiolabeled $^{73}AsO_4$ (Los Alamos National Laboratory) was used in conjunction with liquid scintillation (LS). Ion chromatography (IC) was used (Dionex AS4A-SC) periodically to verify concentrations determined by LS, and to verify that no reduction of AsO_4 to AsO_3 had occurred during the experiments. The purity of the AsO_4 stock solutions was verified by IC.

2.3.2. Kinetic Adsorption Study

A batch study was performed to determine the adsorption kinetics of AsO_4 onto the sand, and to determine an equilibrium time required for batch adsorption isotherm experiments. The kinetic adsorption experiments were performed in 15-mL polyethylene screw top bottles (Nalgene), and consisted of a 1:1 solid to solution ratio (5 g solid:5 mL solution), using initial concentrations of 150 μM AsO_4. All solutions were prepared in a background of 0.01 M KCl. Samples were collected at time intervals of 2, 4, 8, 24, 48, 96, and 168 h, and were decanted and filtered through 0.45μ nylon filters prior to analysis by AA-HG. Adsorbed concentrations were then determined by difference between initial and final measured solute concentrations.

2.3.3. Batch Isotherms

Batch adsorption isotherms for AsO_4 onto the sand were performed in duplicate in 35-mL polypropylene centrifuge tubes (Nalgene), and were performed using a 1:2 solid to solution ratio (5 g solid:10 mL solution). Initial concentrations of 1.33, 4.00, 13.3, 40.0, 133, 400, and 667 μM AsO_4 were used, in a background of 0.01 M KCl. Samples were shaken for 168 h, then decanted and filtered through 0.45μ nylon filters prior to analysis by AA-HG. Adsorbed concentrations were determined by difference between initial and final measured solute concentrations.

2.3.4. Column Transport Experiments

Column transport experiments were performed using 2.8-cm inside diameter, 8-cm length polycarbonate columns containing ~76.5 g sand, resulting in a bulk density of ~1.55 g cm^{-3} and a calculated porosity of ~0.41. The end caps of the columns consisted of fine nylon mesh (<0.1 mm) supported by a Teflon plate drilled with 1-mm holes on 3-mm centers. A syringe pump (Soil Measurement Systems, Tucson, AZ) was used to deliver eluant to the bottom of each column. Four different pore water velocities were established in separate column runs (0.2, 1.0, 10, and 90 cm h^{-1}) using intermittent syringe pump pulses. After initial saturation and conditioning with 0.01 M KCl, approximately 1 pore volume of a tritiated water solution (^3H_2O in 0.01 M KCl background, ~500 Bq mL^{-1}) was pulsed through the columns as a conservative tracer, followed by an eluant of 0.01 M KCl. After complete recovery of the ^3H_2O pulse (~6 pore volumes total flow), one pore volume of 133 μM ^{73}As-labeled AsO_4 (~1650 Bq mL^{-1}, 0.01 M KCl background) was applied followed by 0.01 M KCl. The experiments were continued until the tailing of AsO_4 in column effluent was well established (~20 pore volumes), and AsO_4 concentrations approached baseline levels.

Column effluent was passed through an in-line 0.45μ nylon filter and collected in glass test tubes using a fraction collector (~8 samples per pore volume). Effluent samples were analyzed for pH, followed by ^{73}As activity as determined by LS. Periodic determinations of AsO_4 concentration by IC verified that no reduction of AsO_4 had occurred during transport. After termination, the sand from the columns was extracted with a mixture of 6N HCl and 3N HNO_3 to desorb the remaining sorbed AsO_4, and the resulting extract analyzed for ^{73}As activity using LS to verify complete recovery of all applied As. In all cases, the total recovery of applied As was greater than 95%.

2.3.5. Determination of Column Transport Parameters

The volumes of column effluent samples were determined by mass, and the water flux (q) determined as the average sample volume divided by the collection interval. Pore water velocity (v) was then determined as $q\,\theta^{-1}$ where θ was calculated using the relation $\theta = 1-(\rho/2.65)$, assuming a particle density of 2.65 g cm^{-3} and complete saturation in the columns. Breakthrough curves (BTCs) for ^3H_2O were fitted to the one-dimensional CDE with the computer program CXTFIT (Parker and van Genuchten, 1984) assuming no adsorption of ^3H_2O (retardation factor = 1) to determine column dispersion coefficients (D). All ^3H_2O BTCs were symmetrical, exhibited no tailing, and conformed to the CDE based on the LEA with r^2 values > 0.99. These criteria were used to verify a lack of transport related (physical) nonequilibrium in the column transport experiments (Brusseau, 1992).

2.4. Results

2.4.1. Kinetic Adsorption Study

The kinetics of AsO_4 adsorption onto sand showed that approximately 97% of the equilibrium adsorbed AsO_4 concentration was reached within 24 h (Figure 1). Equilibrium (as defined by constancy of the ratio of adsorbed AsO_4 concentration to aqueous AsO_4

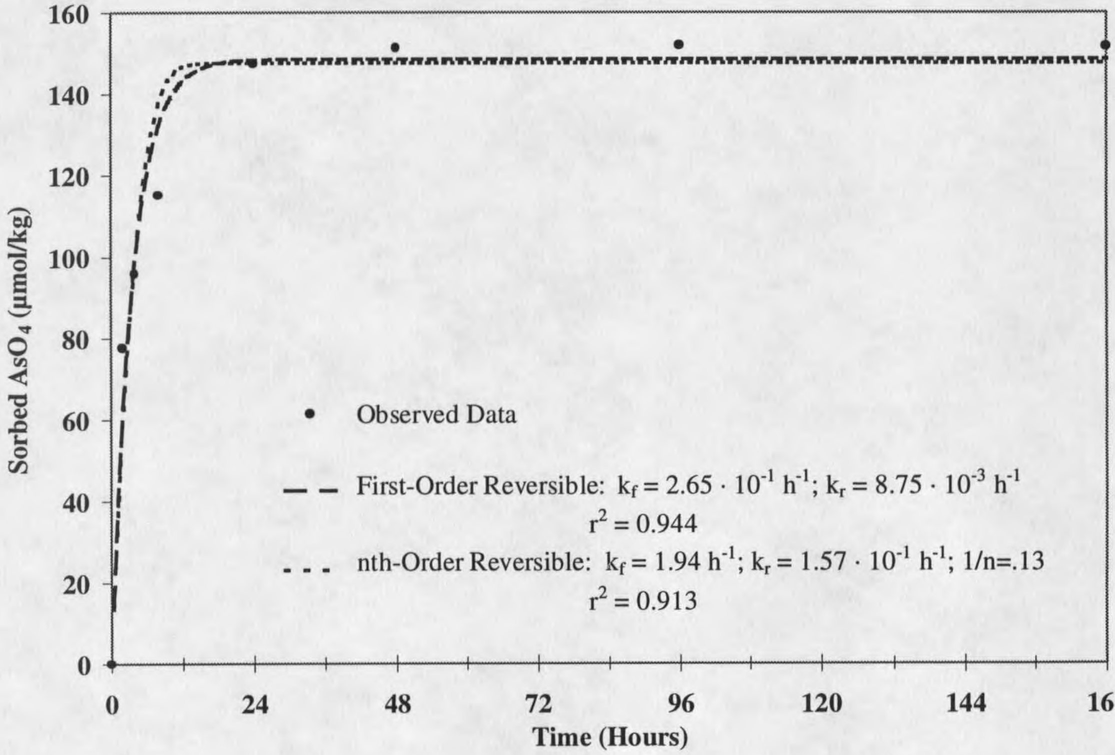

Figure 1: Adsorption kinetics of AsO_4 onto sand and FITMRM model results for first- and nth-order kinetic models. Experimental conditions: 1:1 solid:solution ratio (5 g (dry weight) solid:5 mL solution); pH range = 4 to 5; 150 µM initial AsO_4 in a background solution of 0.01 M KCl.

concentration) was not reached until at least 96 h, which is consistent with other studies showing a slow approach to equilibrium for AsO_4 sorption onto amorphous Al hydroxides (Anderson et al., 1976) and ferrihydrite (Fuller et al., 1993). Since the actual chemical step for the adsorption reaction of AsO_4 onto Fe and Al oxides and clay mineral surfaces has been shown to occur on the order of milliseconds (Grossl, 1995; Amacher et al., 1991; Sparks and Zhang, 1991), the slower approach to equilibrium observed in this experiment suggests that the kinetics of AsO_4 adsorption onto the sand were likely limited by intra or interaggregate diffusional processes.

2.4.2. Batch Adsorption Isotherms

The sorption of AsO_4 onto the sand showed nonlinear behavior above equilibrium solution concentrations of 10 μM AsO_4 (Figure 2). At low As concentrations (< 10 μM AsO_4), the adsorption data was approximately linear; in this range the adsorption data could be described by the linear isotherm (Table 1, Case A), using a $K_D = \sim 200$ L kg^{-1}. The complete set of observed adsorption data were modeled to the best fit (nonlinear regression) Freundlich isotherm (Table 1, Case B), resulting in a $K_F = 24.6$ L kg^{-1} and $1/n=0.13$ ($r^2=0.961$).

2.4.3. Determination of Kinetic Adsorption/Desorption Rate Parameters

In order to determine an independent estimate of kinetic adsorption/desorption rate parameters for use in predictive transport models, the batch kinetic adsorption data (Figure 1) were fit to the first-order reversible and the nth-order reversible adsorption models (Table 1, Cases C and D, respectively) using the computer program FITMRM

(Selim et al., 1990), assuming the presence of a single kinetically limited phase in the sand. For the first-order reversible model, both the forward and reverse rate constants (k_f and k_r, respectively) were allowed to vary independently, resulting in $k_f = 2.65 \times 10^{-1}$ h^{-1} and $k_r = 8.75 \times 10^{-3}$ h^{-1} ($r^2 = 0.944$). The fitted rate constants yield an apparent equilibrium linear distribution coefficient ($K_D' = \frac{\theta\, k_f}{\rho\, k_r}$) at a 1:1 solid:solution ratio of ~30 L kg^{-1}, as compared with the approximated K_D = 200 L kg^{-1} (Figure 2).

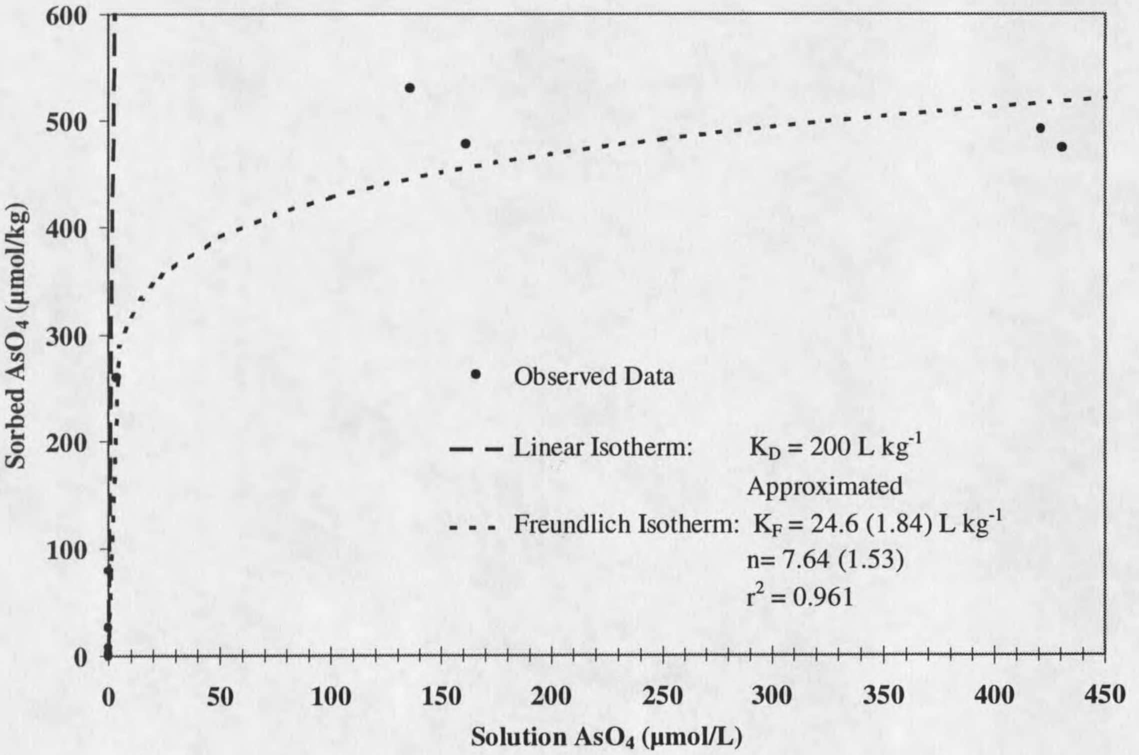

Figure 2: Adsorption isotherms (Background: 0.01 M KCl) for AsO$_4$ at a 1:2 solid:solution ratio (5 g (dry weight) solid:10 mL solution) and a pH range of 4.0 to 4.6. Fitted lines represent (i) the linear isotherm using an approximate K_D of 200 L kg^{-1} to fit the linear portion of the data, and (ii) the Freundlich isotherm where K_F and n were fit using nonlinear regression. Standard errors are presented in parentheses for fit data.

Forward and reverse rate constants (k_f and k_r, respectively) corresponding to the nth-order reversible reaction (Table 1, Case D) were determined by fixing the ratio of k_f/k_r and the reaction order such that the apparent Freundlich equilibrium distribution coefficient ($K_F' = \frac{\theta\, k_f}{\rho\, k_r}$) and the dimensionless Freundlich reaction order (n) were equal to values as determined from batch equilibrium isotherms ($K_F = 24.6\ \mathrm{L\ kg^{-1}}$, $1/n = 0.13$). Nonlinear regression fits resulted in $k_f = 1.94\ \mathrm{h^{-1}}$ and $k_r = 1.57\mathrm{x}10^{-1}\ \mathrm{h^{-1}}$ ($r^2 = 0.913$).

2.4.4. Column Transport Experiments

Column dispersion coefficients were determined from ^3H_2O BTCs using CXTFIT (Parker and van Genuchten, 1984), at pore water velocities of 1 cm h^{-1} (D=0.1058 cm^2 h^{-1}, r^2=0.999), 10 cm h^{-1} (D=0.8305 cm^2 h^{-1}, r^2=0.991), and 90 cm h^{-1} (D=16.31 cm^2 h^{-1}, r^2=0.998), and indicated that no transport related nonequilibrium occurred in the column experiments (Figure 3). ^3H_2O was not used in the slowest pore water velocity (0.2 cm h^{-1}), consequently, no dispersion coefficient was determined for that column experiment. Additional saturated column transport experiments performed in related experiments (Chapter 3) using the same columns and sand under the same packing conditions have all indicated that transport related (physical) nonequilibrium was not important over this range in pore water velocities. The column transport experiments were performed using unbuffered pulse and eluant solutions. Pore water pH, as determined by measurement of effluent samples, fell within the pH range of 4.0 to 4.5 for all transport experiments.